Received: 29 September 2024 | Revised: 14 February 2025 | Accepted: 16 February 2025

DOI: 10.1002/alz.70089

Alzheimer's & Dementia®
THE JOURNAL OF THE ALZHEIMER'S ASSOCIATION

RESEARCH ARTICLE

Decreased water exchange rate across the blood–brain barrier throughout the Alzheimer's disease continuum: Evidence from Chinese data

Guanqun Chen[1] | **Hui Li**[2] | **Xingfeng Shao**[3] | **Danny J. J. Wang**[3] | **Wenli Hu**[1] | **Ying Han**[4,5,6,7,8,9] | **Qi Yang**[2]

[1]Department of Neurology, Beijing Chaoyang Hospital, Capital Medical University, Beijing, China

[2]Department of Radiology, Beijing Chaoyang Hospital, Capital Medical University, Beijing, China

[3]Laboratory of FMRI Technology (LOFT), USC Mark & Mary Stevens Neuroimaging and Informatics Institute, Keck School of Medicine, University of Southern California, Los Angeles, California, USA

[4]Department of Neurology, Xuan Wu Hospital of Capital Medical University, Beijing, China

[5]School of Biomedical Engineering, Hainan University, Haikou, China

[6]Institute of Biomedical Engineering, Shenzhen Bay Laboratory, Gaoke Innovation Center, Shenzhen, China

[7]Center of Alzheimer's Disease, Beijing Institute for Brain Disorders, Beijing, China

[8]National Clinical Research Center for Geriatric Diseases, Beijing, China

[9]The Central Hospital of Karamay, Karamay, China

Correspondence
Ying Han, Department of Neurology, Xuan Wu Hospital of Capital Medical University, No. 45 Changchun Street, Xicheng District, Beijing 100053, China.
Email: hanying@xwh.ccmu.edu.cn

Qi Yang, Department of Radiology, Beijing Chaoyang Hospital, Capital Medical University, No. 8 Gongti South Road, Chaoyang District, Beijing 100020, China.
Email: yangyangqiqi@gmail.com

Funding information
National Natural Science Foundation of China, Grant/Award Numbers: NSFC 82025018, 82020108013, 82327809, 82401661; Sino-German Cooperation, Grant/Award Number: M-0759; Shenzhen Bay Scholars Program and Tianchi Scholars Program; R&D Program of the Beijing Municipal Education Commission, Grant/Award Number: KM202310025013; Beijing Chao-Yang Hospital Multidisciplinary Team Program,

Abstract

INTRODUCTION: Water exchange rate (Kw) across the blood–brain barrier (BBB) is used in magnetic resonance imaging (MRI) techniques to evaluate BBB functionality. Variations in BBB Kw across the Alzheimer's disease (AD) continuum remain uncertain.

METHODS: The study encompassed 38 cognitively normal individuals without AD biomarkers (CN_A–), 30 cognitively normal (CN_A+), and 31 cognitively impaired individuals (CI_A+) with positive AD biomarkers. Participants underwent clinical assessments, MRI/positron emission tomography scans, and assays of plasma biomarkers.

RESULTS: Significantly lower Kw was observed in multiple brain regions throughout the AD continuum. This alteration in Kw correlated with plasma biomarkers and neuropsychological performance. Elevated levels of phosphorylated tau 217 intensified the inverse relationship between Kw and neuropsychological performance. The integration of Kw, brain volume, and plasma biomarkers demonstrated potential in distinguishing stages within the AD continuum.

Guanqun Chen and Hui Li contributed equally to this work.

Grant/Award Numbers: CYDXK202201, CYDXK202207; US National Institutes of Health grant, Grant/Award Number: R01NS114382; the STI2030-Major Projects, Grant/Award Number: 2022ZD0211800

DISCUSSION: Consistently lower Kw was evident across the AD continuum and may act as a diagnostic tool for early AD screening.

KEYWORDS
Alzheimer's disease, biomarker, blood–brain barrier, magnetic resonance imaging, plasma, positron emission tomography, water exchange rate

Highlights

- Observations revealed a decline in water exchange rate (Kw) across multiple brain regions within the Alzheimer's disease (AD) continuum, notably in the hippocampus, parahippocampal gyrus, and deep brain nuclei during the preclinical stage of AD.
- Strong correlations were established between Kw levels in various brain regions and plasma biomarkers, as well as neuropsychological performance in the AD continuum.
- Interaction between plasma phosphorylated tau (p-tau)217 and Kw in the hippocampus was linked to executive function, indicating a combined detrimental impact on cognitive abilities stemming from both blood—brain barrier Kw and p-tau 217.
- The combined use of Kw, brain volume, and plasma biomarkers—neurofilament light chain and glial fibrillary acidic protein—demonstrated potential for distinguishing individuals within the AD continuum.

1 | BACKGROUND

Alzheimer's disease (AD), characterized by progressive deterioration in memory, language, and logical thinking, is the leading cause of dementia.[1] Significant progress has been made in the diagnosis and treatment of AD. According to updated diagnostic criteria, AD exists on a continuum and is defined by its biology, rather than its syndromic presentation.[2] Although the US Food and Drug Administration (FDA) has approved three anti-amyloid monoclonal antibodies aimed at slowing cognitive decline in AD,[3] the safety and efficacy of these immunotherapies with anti-amyloid beta (Aβ) antibodies remain controversial.[4,5] Therefore, identifying new therapeutic targets for AD requires a deeper understanding of its pathogenic mechanisms.

The blood–brain barrier (BBB) is a highly selective, semipermeable interface that protects the central nervous system (CNS) from exposure to toxins and pathogens in the blood.[6] A previous study has shown that BBB breakdown is an early biomarker in individuals with early cognitive dysfunction, independent of Aβ and tau biomarkers.[7] Animal studies have demonstrated interrelationships among BBB dysfunction and Aβ, tau, neuroinflammation, apolipoprotein E (*APOE*) genotype, and aging.[8–10] A recent proof-of-concept trial suggested that aducanumab infusion,combined with focused ultrasound to open the BBB, resulted in a modest reduction in Aβ burden among AD patients.[11] Thus, focusing on BBB dysfunction is crucial for the early detection of AD and the in-depth study of its pathogenic mechanisms.

Traditionally, cerebrospinal fluid (CSF)[12] and dynamic contrast-enhanced magnetic resonance imaging (DCE-MRI)[13] are used to assess BBB integrity in vivo. However, these methods are invasive or have relatively low sensitivity. Furthermore, BBB damage involves not only structural changes but also functional impairment.[14] Recently, non-invasive diffusion-prepared pseudo-continuous arterial spin labeling imaging (DP-pCASL) has been validated to measure the water exchange rate (Kw) across the BBB, offering greater sensitivity in detecting alterations in BBB function.[15] The DP-pCASL technique has been applied to study aging[16–18] and several diseases, including cerebral small vessel disease[19–21] and schizophrenia.[22] These studies demonstrated significant decreases in Kw values throughout the brain and in multiple brain regions, along with significant associations between lower Kw and more severe clinical symptoms and pathophysiological alterations. For example, Gold et al. reported that low Kw across the BBB was associated with lower CSF Aβ42 concentration in normal cognitive aging, suggesting that Kw may be a promising non-invasive indicator of BBB Aβ clearance functions.[16] Furthermore, BBB Kw values in the neocortices differed significantly between groups (*APOE* ε4 non-carriers > heterozygotes > homozygotes). Increased *APOE* ε4 dose is associated with decreased effective brain waste clearance, including iron and Aβ, through the BBB.[23] However, it remains unclear whether BBB damage occurs across the AD continuum in vivo, and whether there is a correlation between BBB damage and AD neuropathologic changes and neuropsychological function.

Here, we used data from a Chinese cohort in Beijing to unveil altered BBB water exchange and highlight the potential of this imaging technique to reflect pathophysiological processes and monitor disease progression from cognitively normal individuals without AD pathology across the AD continuum.

2 | METHODS

2.1 | Participants

A total of 99 subjects from Beijing were included, consisting of 82 subjects from the Sino Longitudinal Study on Cognitive Decline (SILCODE)[24] and 17 from the Beijing Chaoyang Hospital. All subjects underwent physical examinations, MRI evaluations, neuropsychological assessments, and measurements of plasma biomarkers and/or Aβ-positron emission tomography (PET) imaging. Plasma biomarkers included phosphorylated tau (p-tau)217, neurofilament light chain (NfL), and glial fibrillary acidic protein (GFAP).

According to revised criteria for the diagnosis and staging of AD,[2] an abnormal result of the Core 1 biomarker, including Aβ-PET, approved CSF biomarkers, and accurate plasma biomarkers (especially p-tau217), is sufficient to establish a diagnosis of AD. In this study, positive AD biomarkers (A+) were defined as plasma p-tau217 positive and/or Aβ-PET positive, while negative AD biomarkers (A−) were defined as plasma p-tau217 negative and Aβ-PET negative, if available. In cases of conflicting results, Aβ-PET scans were preferred over plasma p-tau217 to determine A+ status.

The diagnosis of cognitively normal (CN) was based on the exclusion of individuals with mild cognitive impairment (MCI) or AD dementia.[25] The cognitive impairment group (CI) included both patients with MCI and mild AD. The dataset comprised 38 CN_A− individuals, 30 CN_A+ individuals, and 31 CI_A+ individuals.

Exclusion criteria included current major psychiatric diagnoses (e.g., major depression or anxiety), other neurological disorders or conditions that can cause cognitive decline (e.g., Parkinson's disease, encephalitis, insomnia, or thyroid dysfunction), inability to complete the study protocol, or any contraindications for MRI (e.g., claustrophobia, cardiac pacemakers, or metal implants). Additionally, participants with outlier values (> 3 standard deviation [SD] from the mean) were excluded.

2.2 | Imaging protocol

MRI data were acquired using a PRISMA 3-Tesla MRI system (Siemens, Erlangen, Germany) with a 64-channel head coil at the Beijing Chaoyang Hospital. Foam padding and earplugs were used to minimize head motion and reduce scanner noise. Participants were instructed to remain still and awake during the scan. High-resolution structural images were acquired using 3D T1-weighted magnetization-prepared rapid gradient echo (MPRAGE). The scan parameters were as follows: repetition time (TR) = 2300 ms, echo time (TE) = 2.98 ms, flip angle (FA) = 9°, slice thickness = 1 mm, field of view (FOV) = 256 × 240 mm^2, and resolution = 1 × 1 × 1 mm^3, 192 slices.

Kw across the BBB was measured using a 3D gradient and spin echo (GRASE) DP-pCASL with the following parameters: resolution = 3.5 ×3.5 × 8 mm^3, TE/TR = 36.3/4200 ms, FA = 120°, FOV = 224 mm × 224 mm, matrix size = 64 × 64, 12 slices (25% oversampling), label/control duration = 1500 ms, centric ordering, and optimized background suppression timing for gray and white matter. A two-stage approach was used during the scan. First, 15 repetitions were acquired during the flow encoding arterial spin tagging (FEAST) scan at post-labeling delay (PLD) = 900 ms and diffusion weighting (b-value) of 0 and 14 s/mm^2 to estimate arterial transit time (ATT). Then, when the labeled blood reached the microvascular compartment, 20 repetitions were acquired at PLD = 1800 ms, with b = 0 and 50 s/mm^2, respectively, to estimate Kw. The total scan duration was 10.01 min.[16]

RESEARCH IN CONTEXT

1. **Systematic review**: We reviewed the literature in PubMed and found that while non-invasive diffusion-prepared pseudo-continuous arterial spin labeling imaging (DP-pCASL) has been used to evaluate water exchange rate (Kw) across the blood–brain barrier (BBB) to detect BBB dysfunction in several diseases, few studies have described the specific alternations of Kw in patients with Alzheimer's disease (AD).
2. **Interpretation**: In this study, significantly lower Kw values were observed in multiple brain regions (gray matter, hippocampus, parahippocampal gyrus, amygdala, temporal lobe, deep brain nuclei, and cingulate cortex) across the AD continuum, and associations were found between Kw in various brain regions and both plasma biomarkers (including phosphorylated tau (p-tau)217 and glial fibrillary acidic protein) and neuropsychological performance across the AD continuum. The integration of the Kw, brain volume, and plasma biomarkers other than p-tau 217 demonstrated potential in distinguishing stages within the AD continuum. These findings suggest that the consistently lower Kw was evident across the AD continuum, and may serve as a useful diagnostic tool for early AD screening.
3. **Future directions**: Future work should focus on mapping the spatiotemporal evolution patterns of the Kw and exploring its relationship with the spread of amyloid beta and tau across the AD continuum.

2.3 | Imaging analysis

The DPpCASL data were postprocessed offline using the LOFT BBB Toolbox (http://www.loft-lab.org/index-5.html), with procedural details as cited previously.[16] Initially, control and label images were corrected for rigid head motion before subtraction to generate perfusion images. Subsequently, the tissue and capillary compartments were delineated from the ASL signal using a diffusion gradient of 50 s/mm^2. The Kw map computation used a total generalized variation (TGV)[26] regularized single-pass approximation (SPA) model, integrating the ASL

signal's tissue or capillary fraction, ATT, T1 of arterial blood (1.66 s), and brain tissue as algorithmic inputs. From background-suppressed control images captured at two PLDs, a voxel-wise tissue T1 map was generated.

Normalization of the Kw maps to the Montreal Neurological Institute (MNI) template was executed using SPM12 (https://www.fil.ion.ucl.ac.uk/spm). Initially, M0 images, located in the same coordinate space as the Kw maps, were co-registered with each participant's T1-weighted images. This was followed by the normalization of the T1-weighted images to the MNI template space. Subsequently, the Kw maps were aligned to the MNI template space using the transformation matrices derived from the normalized T1-weighted images. Post-normalization, mean values in nine regions of interest (ROIs) pertinent to AD were quantified: gray matter (GM), hippocampus, parahippocampal gyrus, amygdala, frontal lobe, parietal lobe (inclusive of both inferior and superior parietal lobule), temporal lobe, cingulate cortex (CC), and deep brain nuclei (DBN, including putamen, caudate, and thalamus). The GM mask was segmented by SPM12, with additional ROIs selected from the Anatomical Labeling Template in SPM12.[27]

Further processing of the 3D T1-weighted images was conducted via the Computational Anatomy Toolbox 12 software (CAT12, http://www.neuro.unijena.de/cat) integrated into SPM12. This included normalization to the standard MNI space, segmentation, and modulation. Volumes for the specified ROIs were extracted. To assess the impact of overall brain size, the brain volume proportion (BVP)—defined as the ratio of brain volume to total intracranial volume (including all CSF, white matter, and GM) for each subject—was calculated.

2.4 | Measurement of AD biomarkers

Plasma levels of p-tau217, NfL, and GFAP were measured by immunoassay, following manufacturer protocols, using an automatic Simoa HD-X analyzer (Quanterix). The methodology for plasma p-tau217 measurement was elaborated in our prior studies.[28,29] Subjects were classified as p-tau217 positive if plasma p-tau217 levels were ≥ 0.661. This threshold was established through receiver operating characteristic curve (ROC, area under the ROC curve [AUC] > 0.8) analysis, using Aβ-PET pathology as the reference standard (unpublished data). Aβ-PET imaging was conducted using ^{18}F-florbetapir (^{18}F-AV-45) at Xuan Wu Hospital, with data acquisition and parameters detailed in previous studies.[28,29] The reconstructed ^{18}F-AV-45 PET images were visually interpreted and categorized as negative or positive by one moderate and one experienced neuroradiologist.[30] In cases of disagreement, a third experienced neuroradiologist adjudicated.

2.5 | Neuropsychological measures

Neuropsychological assessments were structured to evaluate overall cognition and key cognitive domains such as memory, executive function, and language. The evaluations included the basic version of Montreal Cognitive Assessment (MoCA-B), long-term delayed recall from Auditory Verbal Learning Test-Huashan version (N5), recognition (N7), Shape Trail Test A (STT-A), Shape Trail Test B (STT-B), Verbal Fluency Task (VFT), Boston Naming Test (BNT), and Functional Activity Questionnaire (FAQ).

2.6 | Statistical analyses

Statistical analyses were performed using SPSS 26 (IBM). Continuous variables, including demographic data and plasma biomarkers, were expressed as mean ± SD and analyzed using one-way analysis of variance with post hoc tests. Sex data were expressed as counts and analyzed using chi-square tests.

Kw values were compared among the CN_A+ group, CI_A+ group, and the CN_A− group using linear regression analysis with age, sex, education, BVP, and group as independent variables, and Kw as the dependent variable. A Bonferroni correction was used to adjust for multiple comparisons. Subsequent correlation analyses focused on ROIs demonstrating significant differences between groups. Partial correlation analysis was conducted to explore potential relationships among Kw, plasma biomarkers, and neuropsychological scores, adjusting for age, sex, and education level.

Moderation analysis used PROCESS (version 4.2)[31] to investigate the effect of plasma p-tau217 on the relationship between Kw and neuropsychological scores. In this model, *z*-transformed Kw values were considered independent variables, *z*-transformed neuropsychological scores were the dependent variables, and *z*-transformed plasma p-tau217 was evaluated as a potential moderator. Johnson–Neyman analyses were conducted to identify significant moderation thresholds. All analyses were executed using R statistical software (R Core Team, 2014) and SPSS 26.

Finally, ROC analysis with SPSS 26 calculated the sensitivity and specificity of imaging and plasma biomarkers for differentiating among the CN_A−, CN_A+, and CI_A+ groups. ROC curves were analyzed for the combined Kw that exhibited significant between-group differences, as well as combinations of Kw, BVP, NfL, and GFAP.

3 | RESULTS

3.1 | Subject characteristics

The demographic and clinical characteristics of the subjects are presented in Table 1. There were no significant differences in age and sex among the three groups. However, significant differences were observed in years of education ($p = 0.006$) and all neuropsychological scores ($p < 0.001$ for all). The CI_ A+ group had fewer years of education compared to the other two groups (CN_A−, $p = 0.002$; CN_A+, $p = 0.025$) and scored lower on all tests assessing global cognition, memory, executive function, language function, and functional activities (CN_A−, $p < 0.001$ for all; CN_A+, $p < 0.001$ for all), with no significant differences noted between CN_A− and CN_A+.

TABLE 1 Demographic information and plasma biomarkers in the three groups.

	CN_A− (*n* = 38)	CN_A+ (*n* = 30)	CI_A+ (*n* = 31)	*p*
Sex (M/F)	17/21	9/21	9/22	0.304
Age (years)	68.785 ± 4.838	70.266 ± 6.942	67.741 ± 8.164	0.336
Edu (years)	15.184 ± 3.958	14.366 ± 4.156	11.887 ± 4.664	0.006[b,c]
MoCA-B	26.000 ± 1.724	26.433 ± 2.112	14.935 ± 5.680	<0.001[b,c]
N5	6.289 ± 2.459	6.500 ± 2.713	1.548 ± 2.157	<0.001[b,c]
N7	21.078 ± 3.671	22.000 ± 1.838	8.225 ± 5.655	<0.001[b,c]
STT-A	53.578 ± 13.747	60.733 ± 23.106	132.548 ± 84.247	<0.001[b,c]
STT-B	130.184 ± 38.363	144.600 ± 43.064	227.225 ± 90.065	<0.001[b,c]
BNT	26.657 ± 1.681	25.500 ± 2.556	18.774 ± 5.572	<0.001[b,c]
VFT	21.289 ± 2.930	20.400 ± 5.021	8.612 ± 3.431	<0.001[b,c]
FAQ	0.894 ± 1.797	0.433 ± 0.858	10.322 ± 6.425	<0.001[b,c]
Plasma p-tau217	0.258 ± 0.089	0.677 ± 0.364	0.980 ± 0.508*	<0.001[a,b,c]
Plasma NfL	13.425 ± 5.546	19.225 ± 9.084	26.082 ± 21.131*	0.001[a,b]
Plasma GFAP	90.705 ± 32.016	148.241 ± 71.014	199.187 ± 99.556*	<0.001[a,b,c]

Note: Continuous variables are expressed as mean ± standard deviation, and sex as numbers (male/female).
Abbreviations: A−, with negative Alzheimer's disease biomarkers; A+, with positive Alzheimer's disease biomarkers; BNT, Boston Naming Test; CI, cognitively impaired; CN, cognitively normal; FAQ, Functional Activity Questionnaire; GFAP, glial fibrillary acidic protein; MoCA-B, basic version of Montreal Cognitive Assessment; N5, long-term delayed recall; N7, long-term delayed recognition; NfL, neurofilament light chain; p-tau, phosphorylated tau; STT-A, Shape Trail Test A; STT-B, Shape Trail Test B; VFT, Verbal Fluency Task.
*Only 13 subjects in the CI_A+ group have plasma biomarker values; others are diagnosed using amyloid beta-positron emission tomography.
[a]Statistical significance ($p < 0.05$) between CN_A− and CN_A+.
[b]Statistical significance ($p < 0.05$) between CN_A− and CI_A+.
[c]Statistical significance ($p < 0.05$) between CN_A+ and CI_A+.

Regarding plasma biomarkers, it is noted that all subjects in the CN_A− and CN_A+ groups had plasma biomarker values, whereas only 13 subjects in the CI_A+ group had these values, with others diagnosed using Aβ-PET. Significant differences were found in levels of p-tau217 ($p < 0.001$), NfL ($p = 0.001$), and GFAP ($p < 0.001$) among the groups. The CN_A+ group exhibited higher levels of p-tau217 ($p < 0.001$), NfL ($p = 0.029$), and GFAP ($p < 0.001$) compared to the CN_A− group, while the CI_A+ group showed higher levels of p-tau217 ($p < 0.001$), NfL ($p < 0.001$), and GFAP ($p < 0.001$) compared to the CN_A−. Furthermore, the CI_A+ group had significantly higher levels of p-tau217 ($p = 0.004$) and GFAP ($p = 0.016$) than the CN_A+ group. Additionally, 54 of the 99 individuals underwent Aβ-PET examination, including 7 Aβ (−) individuals in the CN_A− group, 24 Aβ (+) individuals in the CN_A+ group, and 23 Aβ (+) individuals in the CI_A+ group.

3.2 | Comparison of Kw among the CN_A−, CN_A+, and CI_ A+ groups

As indicated in Table 2, linear regression analyses, adjusted for age, sex, and education, showed lower Kw values in the CN_A+ group compared to the CN_A− group in the hippocampus ($p = 0.020$), parahippocampal gyrus ($p = 0.035$), and DBN ($p = 0.029$), although these *p* values did not withstand Bonferroni correction. In contrast, the CI_A+ group exhibited significantly lower Kw in the GM, hippocampus, parahippocampal gyrus, amygdala, temporal lobe, CC, and DBN compared to the CN_A− group ($p = 0.002$ for amygdala, $p = 0.001$ for CC, $p < 0.001$ for all other regions). A schematic representation of the between-group differences in the whole brain was illustrated in Figure 1A.

Given the relevance of brain atrophy in AD, a one-way analysis of variance was conducted to examine group differences in BVP, and Pearson correlation analysis assessed the relationship between Kw and BVP within the same ROIs. Significant differences in BVP were observed in GM, hippocampus, parahippocampal gyrus, amygdala, frontal lobe, parietal lobe, temporal lobe, and CC among the three groups (Table S1 in supporting information). Significant correlations between BVP and Kw were found in GM, hippocampus, parahippocampal gyrus, temporal lobe, amygdala, DBN, and CC (Table S2 in supporting information). Subsequent linear regression analyses, controlling for BVP in these seven ROIs showing significant group differences and significant correlations between BVP and Kw, were performed. Bonferroni correction adjusted for multiple comparisons ($p = 0.05/7 = 0.0071$). The results demonstrated that, after adjusting for age, sex, education, and BVP, the CN_A+ group had lower Kw in the hippocampus ($\beta = -9.621$ $p = 0.032$; Figure 1C), though this did not meet the Bonferroni correction threshold. In contrast, the CI_A+ group showed significantly lower Kw in GM ($\beta = -13.904$ $p = 0.007$;

TABLE 2 Comparison of Kw (min^{-1}) among CN_A+, CI_A+, and CN_A−, adjusted for age, sex, and education.

				CN_A− vs. CN_A+		CN_A+ vs. CI_A+	
Brain regions	**CN_A− ($n = 38$)**	**CN_A+ ($n = 30$)**	**CI_A+ ($n = 31$)**	***β***	***p***	***β***	***p***
Gray matter	104.151 ± 15.408	97.311 ± 18.523	88.837 ± 20.232	−6.816	0.123	−18.492	<0.001*
Hippocampus	112.857 ± 17.427	102.405 ± 17.476	96.218 ± 20.307	−10.360	**0.020**	−20.738	<0.001*
Parahippocampal gyrus	96.972 ± 18.547	87.662 ± 17.939	78.089 ± 23.626	−10.342	**0.035**	−23.848	<0.001*
Amygdala	122.428 ± 20.971	115.291 ± 19.996	105.197 ± 30.429	−6.707	0.264	−19.846	0.002*
Frontal lobe	99.810 ± 18.528	93.960 ± 19.860	90.846 ± 20.324	−6.511	0.178	−12.485	0.014
Parietal lobe	90.246 ± 24.161	85.812 ± 26.755	74.501 ± 24.713	−3.164	0.613	−16.657	0.012
Temporal lobe	103.508 ± 16.140	97.365 ± 19.451	84.104 ± 20.748	−6.459	0.152	−23.312	<0.001*
Deep brain nuclei	107.861 ± 14.745	98.437 ± 16.721	94.409 ± 20.512	−9.438	**0.029**	−16.374	<0.001*
Cingulate cortex	121.060 ± 16.864	116.127 ± 26.442	105.449 ± 29.658	−5.550	0.352	−20.645	0.001*

Notes: Kw (min^{-1}) are expressed as mean ± standard deviation. Bold *p* values indicate $p < 0.05$, but cannot survive the Bonferroni correction.
Abbreviations: A−, with negative Alzheimer's disease biomarkers; A+, with positive Alzheimer's disease biomarkers; CI, cognitively impaired; CN, cognitively normal.
*Significant *p* value after Bonferroni correction ($p < 0.05/9 = 0.0055$).

Figure 1B), hippocampus ($\beta = -16.322$ $p = 0.007$; Figure 1C), and DBN ($\beta = -12.501$ $p = 0.006$; Figure 1D).

3.3 | Associations between Kw with plasma biomarkers and neuropsychological scores in participants with plasma biomarkers

We explored the correlations of Kw in ROIs with significant group differences—namely GM, hippocampus, and DBN—with plasma biomarkers and neuropsychological scores in participants who had plasma biomarkers ($n = 81$). Statistical significance for partial correlation analysis between Kw and plasma biomarkers was set at $p < 0.05/$(number of ROI × number of plasma markers) = 0.05/9 = 0.0055. Statistical significance for partial correlation analysis between Kw and neuropsychological scores was set at $p < 0.05/$(number of ROI × number of neuropsychological scores) = 0.05/24 = 0.0021. Results indicated that lower Kw in the hippocampus was significantly associated with higher levels of p-tau217 ($r = -0.396$, $p < 0.001$; Figure 2A) and GFAP ($r = -0.439$, $p < 0.001$; Figure 2B). Additionally, lower Kw in DBN correlated significantly with increased p-tau217 ($r = -0.319$, $p = 0.004$; Figure 2C) and GFAP ($r = -0.391$, $p < 0.001$; Figure 2D). Furthermore, lower Kw in the hippocampus also correlated significantly with lower MoCA-B scores ($r = 0.429$, $p < 0.001$; Figure 2E), higher STT-A ($r = -0.451$, $p < 0.001$; Figure 2F), and higher STT-B scores ($r = -0.361$, $p = 0.001$; Figure 2G).

3.4 | Associations between Kw with plasma biomarkers and neuropsychological scores in AD participants with plasma biomarkers

In AD participants with plasma biomarkers ($n = 43$), lower Kw in the hippocampus was associated with higher levels of NfL ($r = -0.382$, $p = 0.015$) and GFAP ($r = -0.335$, $p = 0.035$). Lower Kw in DBN was associated with higher GFAP levels ($r = -0.365$, $p = 0.021$). Lower Kw in the hippocampus was correlated significantly with lower MoCA-B scores ($r = 0.394$, $p = 0.012$). However, these *p* values did not meet the Bonferroni correction threshold. Conversely, lower Kw in the hippocampus was significantly associated with higher STT-A scores ($r = -0.462$, $p = 0.002$; Figure 2H).

3.5 | Moderation analyses in AD participants with plasma biomarkers

Moderation analysis revealed a significant interactive effect of p-tau217 × Kw in the hippocampus on STT-A scores (Figure 3A and Table 3). The Johnson–Neyman plot illustrated the range of p-tau217 values at which the effect of Kw on STT-A was statistically significant. For the hippocampus–STT-A relationship, the Johnson–Neyman threshold for p-tau217 was 0.761 (Figure 3B). Above this threshold, higher p-tau217 amplified the negative impact of Kw on STT-A.

3.6 | Discriminative power of the Kw among CN_A−, CN_A+, and CI_ A+ groups

We evaluated the discriminative capability of combined Kw in gray matter, hippocampus, and DBN to distinguish individuals among any two of the three groups. The combined Kw demonstrated good discriminative ability, distinguishing between the CN_A− and CN_A+ group, the CN_A+ and CI_ A+ group, the CN_A− and CI_ A+ group with AUCs of 0.669 (95% confidence interval: 0.536–0.802; Figure 4A), 0.626 (95% confidence interval: 0.437–0.814; Figure 4B), and 0.779 (95% confidence interval: 0.609–0.950; Figure 4C), respectively. Additionally, the accuracy of classification improved when combining Kw, BVP, NfL, and GFAP, showing AUCs of 0.804 (95% confidence interval:

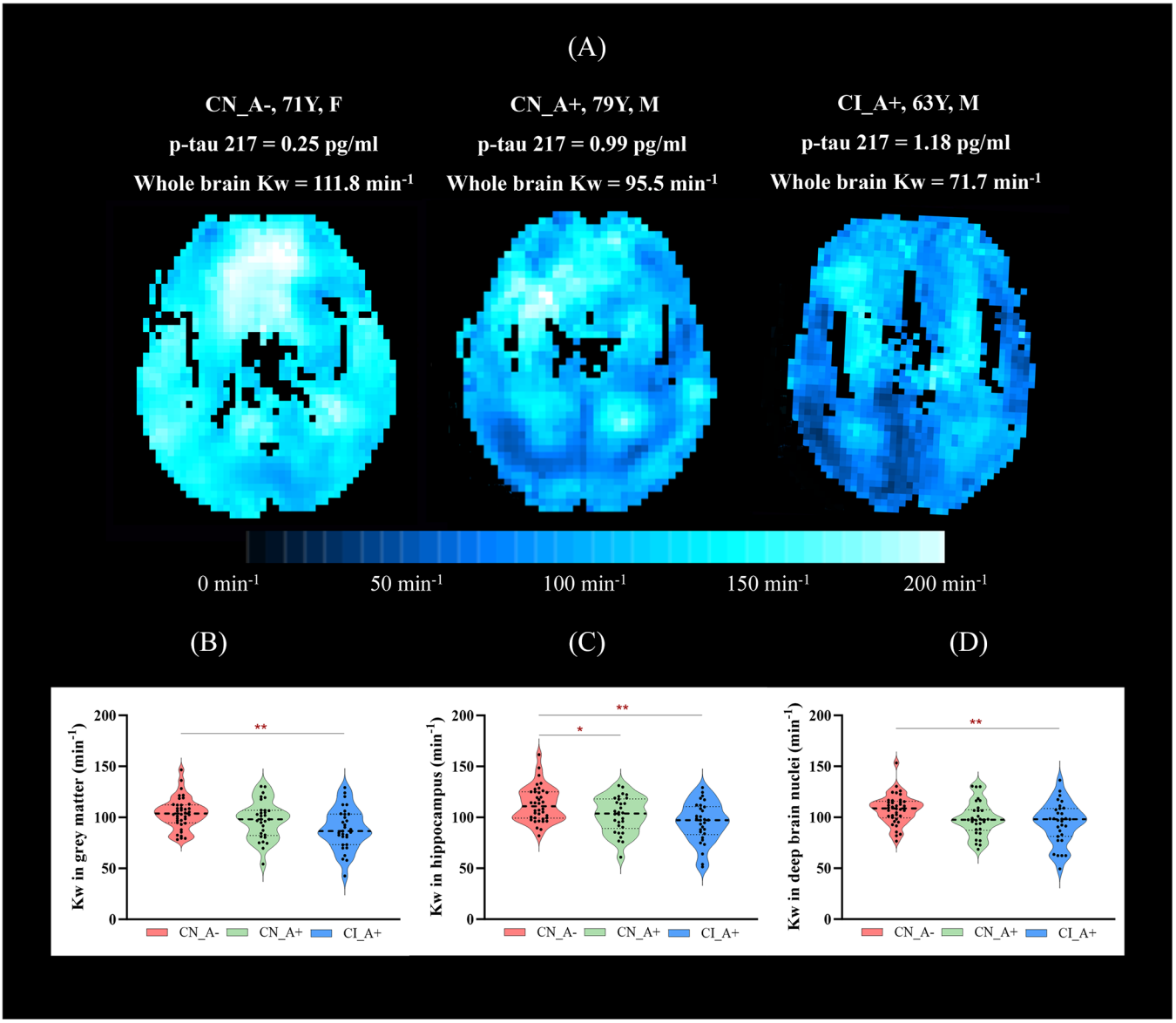

FIGURE 1 Lower Kw in multiple brain regions in CN_A+ and CI_A+, compared to CN_A−. A, Maps of Kw in the whole brain from three representative participants show a trend of lower Kw values in CN_A+ and CI_A+. B, Lower Kw in gray matter in the CI_A+ group compared to the CN_A− group. C, Lower Kw in the hippocampus in the CN_A+ and CI_A+ groups compared to the CN_A− group. D, Lower Kw in deep brain nuclei in the CI_A+ group compared to the CN_A− group. * $p < 0.05$, ** Significant p value after Bonferroni correction ($p < 0.05/7 = 0.0071$). A−, with negative Alzheimer's disease biomarkers; A+, with positive Alzheimer's disease biomarkers; CI, cognitively impaired; CN, cognitively normal; Kw, blood–brain barrier water exchange rate.

0.696–0.911; Figure 4A), 0.810 (95% confidence interval: 0.634–0.987; Figure 4B), and 0.874 (95% confidence interval: 0.713–0.999; Figure 4C) for the respective group comparisons.

4 | DISCUSSION

The main findings of our study are as follows: (1) significantly lower Kw values were found in multiple brain regions in the CN_A+ and CI_A+ groups, compared to the CN_A− group; (2) associations were observed between Kw in multiple brain regions and plasma biomarkers as well as neuropsychological performance across the AD continuum; (3) higher levels of p-tau217 strengthened the negative relationship between Kw in the hippocampus and neuropsychological performance in subjects with AD (CN_A+ and CI_ A+ group); (4) the combination of Kw, BVP, and plasma biomarkers showed potential for distinguishing individuals across the AD continuum.

In our study, we found that, compared to the CN_A− group, the CI_ A+ group exhibited widespread low Kw values in gray matter, hippocampus, parahippocampal gyrus, amygdala, temporal lobe, DBN, and CC. The low Kw in the CN_A+ group was confined to the hippocampus, parahippocampal gyrus, and DBN. These results suggest

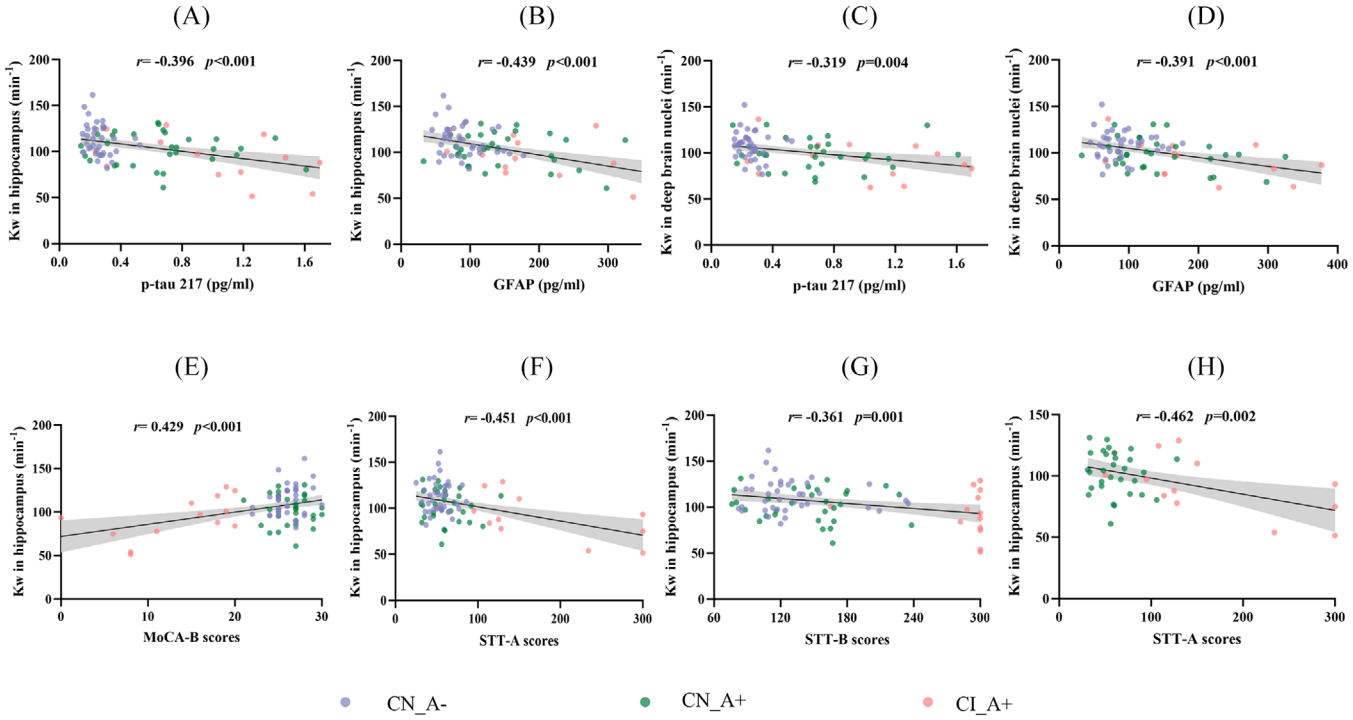

FIGURE 2 Correlations of Kw values in different brain regions with plasma biomarkers and neuropsychological scores. A–D, Significant correlations between Kw in the hippocampus and deep brain nuclei with p-tau217 and GFAP in all participants with plasma biomarkers ($n = 81$). E–G, Significant correlations between Kw in the hippocampus with MoCA-B, STT-A, and STT-B scores in all participants with plasma biomarkers ($n = 81$). H, Significant correlations between Kw in the hippocampus and STT-A scores in AD participants with plasma biomarkers ($n = 43$). AD, Alzheimer's disease; GFAP, glial fibrillary acidic protein; MoCA-B, basic version of the Montreal Cognitive Assessment; p-tau, phosphorylated tau; STT-A, Shape Trail Test A; STT-B, Shape Trail Test B.

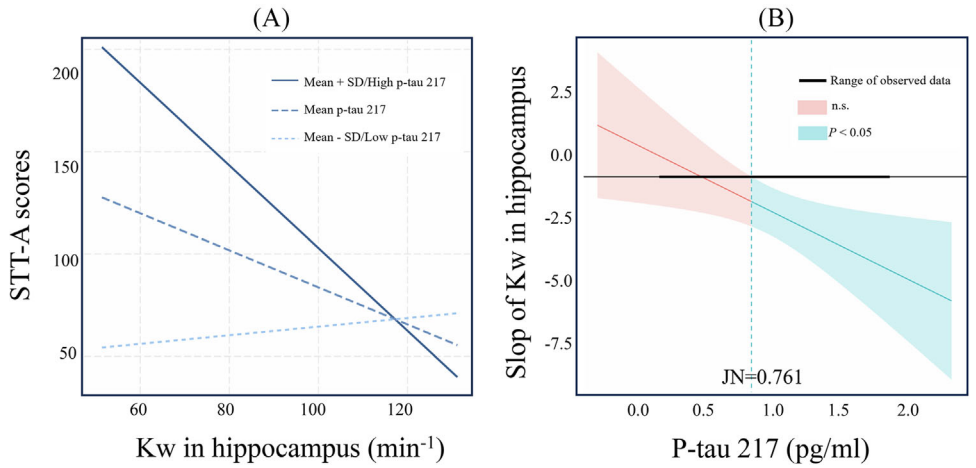

FIGURE 3 The interaction effect of plasma p-tau217 with Kw in the hippocampus on STT-A in AD participants with plasma biomarkers. A, Graph of the simple slope plot showing the interaction between plasma p-tau217 and Kw in the hippocampus on STT-A. B, Graph of the Johnson–Neyman plot showing the conditional effect of Kw (X) on STT-A (Y) as a linear function of plasma p-tau217 (W), including the Johnson–Neyman transition point (i.e., where the confidence interval around the conditional effect crosses zero on the *y* axis). AD, Alzheimer's disease; A–, with negative Alzheimer's disease biomarkers; A+, with positive Alzheimer's disease biomarkers; CI, cognitively impaired; CN, cognitively normal; JN, Johnson–Neyman; Kw, blood–brain barrier water exchange rate; p-tau, phosphorylated tau; SD, standard deviation; STT-A, Shape Trail Test A.

TABLE 3 Moderation effects of Kw (predictor) and p-tau217 (moderator) on STT-A (dependent variable) in AD participants.

Hippocampus	β	95% CI		p	Over R^2
Kw × p-tau217	−0.321	−0.582	−0.058	0.017	0.533
Kw	−0.260	−0.513	−0.006	0.044	
p-tau217	0.283	0.148	0.552	0.039	

Note: Kw, independent variable; STT-A, dependent variable; p-tau217, moderator.

Abbreviations: AD, Alzheimer's disease; CI, confidence interval; Kw, blood-brain barrier water exchange rate; p-tau, phosphorylated tau; STT-A, Shape Trail Test A.

that BBB function is impaired across the AD continuum, with the degree of damage corresponding to the severity of AD. Specifically, the data indicate that BBB dysfunction is more widespread in the later stages of AD and may also be present in preclinical AD. Previous *post mortem* studies have confirmed BBB dysfunction in AD patients.[32,33] However, characterizing BBB impairment and its temporal and spatial evolution across the AD continuum using autopsy specimens is challenging. With the rapid advancement of neuroimaging technology, MRI now enables the in vivo monitoring and evaluation of BBB dysfunction across the AD continuum. DCE-MRI, which uses a paramagnetic gadolinium-based contrast agent, is the most widely used method for quantifying BBB breakdown in clinical settings.[34] Numerous studies based on DCE-MRI have shown that, compared to control subjects, patients in the prodromal and later stages of AD experience significantly increased BBB leakage in several brain regions, including the hippocampus, total GM, and cortex, which correlates with cognitive decline.[35–37] In contrast, DP-pCASL is an imaging technique that uses endogenous water molecules as contrast agents, allowing non-invasive evaluation of water exchange across the BBB with greater sensitivity to early-stage disease.[15] However, limited research has used DP-pCASL to describe BBB damage characteristics in cognitive aging.[18] Several studies have also shown that BBB Kw correlates with neuropsychological performance across multiple brain regions.[16,17] Therefore, the results of this study align with previous findings demonstrating BBB dysfunction in the later symptomatic stages of AD and further expand our understanding of BBB dysfunction across the AD continuum. In this study, we also considered the effects of brain atrophy on BBB Kw. We found that, compared to the CN_A– group, the CI_ A+ group showed lower Kw in gray matter, hippocampus, and DBN. Importantly, the lower Kw in the hippocampus was still evident in the CN_A+ group after adjusting for BVP. The observed contribution of cerebral atrophy to Kw changes with AD progression may result from compromised BBB integrity with neurodegeneration.[18] However, the precise mechanisms need to be confirmed by further basic research and longitudinal clinical studies on the causal relationship between BBB dysfunction and neurodegeneration. These preliminary results suggest that DP-pCASL could help identify key brain regions vulnerable to AD, highlighting its potential as a biomarker for neuropathological changes and cognitive impairment across the AD continuum.

The results of the correlation analysis showed that decreases in Kw in multiple brain regions relevant to AD, such as the hippocampus and DBN, were correlated with high levels of plasma biomarkers (including p-tau217, GFAP, and NfL) across the AD continuum. Although the specific molecular pathway for water exchange across the BBB remains unclear, aquaporin-4 (AQP4) is believed to play a key role. In the CNS, AQP4 is primarily distributed in a polarized pattern in the endfeet of astrocytes, which form an important component of the BBB between the blood and brain parenchyma.[38] The polarized expression of AQP4 on astrocytes facilitates water transport, and thus, the water exchange

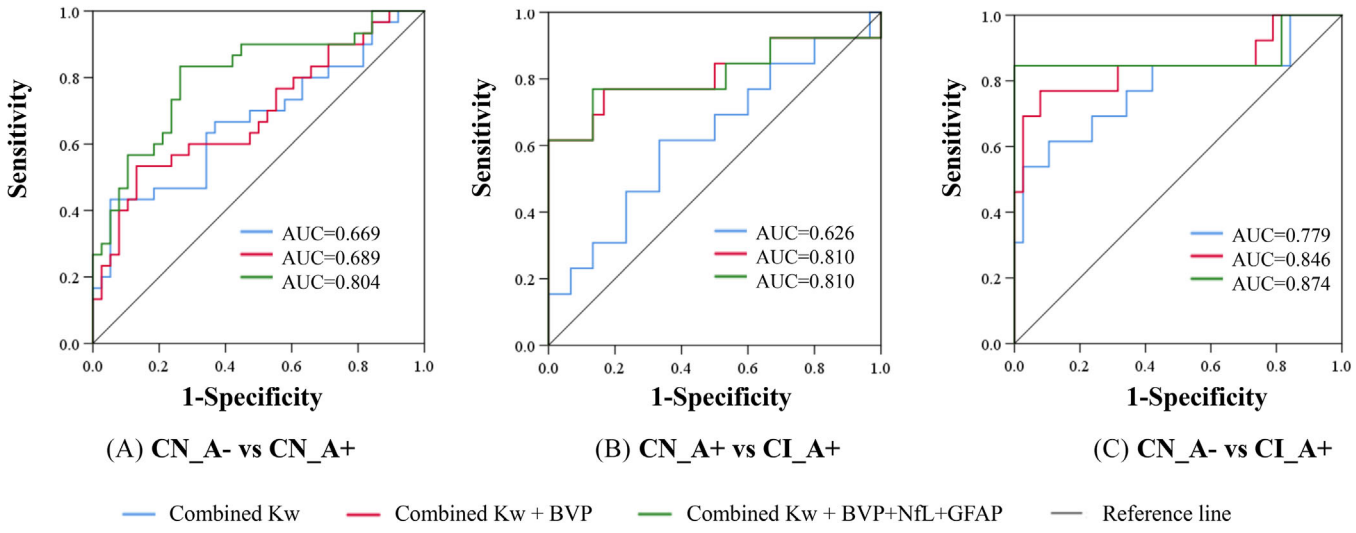

FIGURE 4 Receiver operating characteristic curve. The combination of Kw (gray matter, hippocampus, and deep brain nuclei), BVP, NfL, and GFAP showed relatively higher classification accuracy in classifying individuals between the CN_A– and CN_A+ groups, CN_A+ and CI_ A+ groups, and CN_A– and CI_ A+ groups. A–, with negative Alzheimer's disease biomarkers; A+, with positive Alzheimer's disease biomarkers; AUC, area under the receiver operating characteristic curve; BVP, brain volume proportion; CI, cognitively impaired; CN, cognitively normal; GFAP, glial fibrillary acidic protein; Kw, blood–brain barrier water exchange rate; NfL, neurofilament light chain.

rate across the BBB is lower when AQP4 expression or polarization decreases.[39] Both animal[40] and human autopsy studies[41] have shown a loss of perivascular AQP4 localization in the endfoot membranes, with altered AQP4 expression associated with increased amyloid deposits. Recent studies have demonstrated that plasma p-tau217 performs best for detecting Aβ pathophysiology and shows a substantial increase in AD patients.[42–44] As a result, the high-performance plasma test for p-tau217 was recently classified as a core biomarker for detecting AD neuropathologic change (ADNPC) and diagnosing AD by the Alzheimer's Association Workgroup.[2] Therefore, we speculate that the negative correlation between Kw in the hippocampus, DBN, and p-tau217 may indicate that the lower BBB water exchange rate is related to AQP4 depolarization caused by severe AD pathology. Similarly, NfL[45] and GFAP[46] reflect non-specific processes involved in AD pathophysiology and are promising non-invasive biomarkers for AD. According to the latest revised criteria for diagnosing and staging AD,[2] NfL is a marker of injury, dysfunction, or degeneration of neuropil, while GFAP is a marker of inflammatory/immune processes primarily driven by activated microglia, which are associated with BBB damage.[10,47] Therefore, the correlation between decreased Kw in the hippocampus, DBN, and high levels of NfL and GFAP may suggest that the lower BBB water exchange rate also reflects, at least in part, non-specific pathological processes involved in AD. However, these findings should be further validated in larger scale studies. We also found that decreased Kw in the hippocampus was significantly associated with poorer neuropsychological performance (measured withSTT-A/B and MoCA-B). Additionally, results from moderation analyses suggest that higher levels of p-tau217 further enhanced the negative relationship between Kw in the hippocampus and neuropsychological performance (measured with STT-A) in subjects with AD (CN_A+ and CI_ A+ group). These results suggest that measures of the Kw across the BBB may help identify AD neuropathologic change and cognitive decline across the AD continuum.

In this study, we also evaluated the discriminative power of combined Kw in gray matter, hippocampus, and DBN for distinguishing individuals between any two groups in the AD continuum. The combined Kw demonstrated relatively good discriminative power in classifying individuals between the CN_A– and CN_A+ groups, the CN_A+ and CI_ A+ groups, the CN_A– and CI_ A+ groups, with AUCs of 0.669, 0.626, and 0.779, respectively. Furthermore, the combination of Kw in multiple brain regions and BVP showed higher classification accuracy. When combined, Kw, BVP, NfL, and GFAP achieved higher diagnostic accuracy, particularly for distinguishing individuals between the CN_A– and CI_A+ groups (AUC = 0.874). These results suggest that combining Kw, BVP, and peripheral blood biomarkers other than p-tau217 may offer a valuable tool for identifying individuals across the AD continuum.

A strength of this study is that we used the Core 1 biomarkers to define AD biologically, based on the current revised criteria for AD diagnosis. However, this study has several limitations. First, as a cross-sectional design, it limits our ability to establish causal relationships. Future studies should evaluate the association between Kwacross the BBB, plasma biomarkers, and neuropsychological performance longitudinally. Second, this is a preliminary, single-center study with a relatively small sample size, which may affect the generalizability of the findings. Multicenter data from different regions and ethnicities should be included in future studies. Third, it is crucial to characterize the spatiotemporal evolution patterns of water exchange across the BBB and its relationship with the spread of Aβ, tau, and other neuropathologic changes in the AD continuum. However, not all participants had Aβ-PET data in this study, and data collection on tau-PET is ongoing. Therefore, future studies should incorporate Aβ/tau-PET data and other neuropathologic changes to provide a more comprehensive and in-depth investigation.

In conclusion, this study characterized changes in the Kw across the BBB estimated with the DP-pCASL technique in individuals across the AD continuum and further explored the association among Kw, plasma biomarkers, and neuropsychological performance. Our results suggest that Kw measured by DP-pCASL shows promise as a biomarker for reflecting pathophysiological processes and monitoring cognitive decline across the AD continuum.

ACKNOWLEDGMENTS

The authors would like to express their sincere gratitude to all the participants and investigators involved in this study. The authors would also like to thank their colleagues from Xuan Wu Hospital, Capital Medical University, for their significant contributions to data collection: Mingkai Zhang, Min Wei, Ruixian Li, Xuanqian Wang, Yongzhe Wei, Jie Yang, and Shuyu Zhang. Additionally, the authors thank Dr. Lu Yan (College of Foreign Languages, Beijing University of Technology) for polishing up the manuscript. This study was supported by grants from the National Natural Science Foundation of China (NSFC 82025018, 82020108013, 82327809, 82401661), the STI2030-Major Projects (2022ZD0211800), the Sino-German Cooperation Grant (M-0759), the Shenzhen Bay Scholars Program and Tianchi Scholars Program, the R&D Program of the Beijing Municipal Education Commission (KM202310025013), and the Beijing Chao-Yang Hospital Multidisciplinary Team Program (CYDXK202201, CYDXK202207). This study was also supported by US National Institutes of Health grant R01NS114382.

CONSENT STATEMENT

This study was approved by the Medical Ethics Committee of the Beijing Chaoyang Hospital and Xuan Wu Hospital of Capital Medical University and conducted in accordance with the Declaration of Helsinki. All participants or their family members provided written informed consent and authorized the publication of their clinical details.

CONFLICT OF INTEREST STATEMENT

The authors report no competing interests. Author disclosures are available in the supporting information.

ORCID

Qi Yang https://orcid.org/0000-0002-5773-0456

REFERENCES

1. Sabayan B, Sorond F. Reducing risk of dementia in older age. *JAMA*. 2017;317:2028. doi:10.1001/jama.2017.2247
2. Jack CJ, Andrews JS, Beach TG, et al. Revised criteria for diagnosis and staging of Alzheimer's disease: Alzheimer's Association Workgroup. *Alzheimers Dement*. 2024;20:5143-5169. doi:10.1002/alz.13859
3. Cummings J, Zhou Y, Lee G, Zhong K, Fonseca J, Cheng F. Alzheimer's disease drug development pipeline: 2024. *Alzheimers Dement (N Y)*. 2024;10:e12465. doi:10.1002/trc2.12465
4. The L. Lecanemab for Alzheimer's disease: tempering hype and hope. *Lancet*. 2022;400:1899. doi:10.1016/S0140-6736(22)02480-1
5. Mahase E. Lecanemab: European Drug agency rejects Alzheimer's drug amid debate over efficacy and safety. *BMJ (Online)*. 2024;386:q1692. doi:10.1136/bmj.q1692
6. Wu D, Chen Q, Chen X, Han F, Chen Z, Wang Y. The blood-brain barrier: structure, regulation, and drug delivery. *Signal Transduct Target Ther*. 2023;8:217. doi:10.1038/s41392-023-01481-w
7. Nation DA, Sweeney MD, Montagne A, et al. Blood–brain barrier breakdown is an early biomarker of human cognitive dysfunction. *Nat Med*. 2019;25:270-276. doi:10.1038/s41591-018-0297-y
8. Liebner S, Dijkhuizen RM, Reiss Y, Plate KH, Agalliu D, Constantin G. Functional morphology of the blood–brain barrier in health and disease. *Acta Neuropathol*. 2018;135:311-336. doi:10.1007/s00401-018-1815-1
9. Nehra G, Bauer B, Hartz A. Blood-brain barrier leakage in Alzheimer's disease: from discovery to clinical relevance. *Pharmacol Ther*. 2022;234:108119. doi:10.1016/j.pharmthera.2022.108119
10. Chen Y, He Y, Han J, Wei W, Chen F. Blood-brain barrier dysfunction and Alzheimer's disease: associations, pathogenic mechanisms, and therapeutic potential. *Front Aging Neurosci*. 2023;15:1258640. doi:10.3389/fnagi.2023.1258640
11. Rezai AR, D'Haese PF, Finomore V, et al. Ultrasound blood-brain barrier opening and aducanumab in Alzheimer's disease. *N Engl J Med*. 2024;390:55-62. doi:10.1056/NEJMoa2308719
12. Musaeus CS, Gleerup HS, Hasselbalch SG, Waldemar G, Simonsen AH. Progression of blood-brain barrier leakage in patients with Alzheimer's disease as measured with the cerebrospinal fluid/plasma albumin ratio over time. *J Alzheimers Dis Rep*. 2023;7:535-541. doi:10.3233/ADR-230016
13. Moyaert P, Padrela BE, Morgan CA, et al. Imaging blood-brain barrier dysfunction: a state-of-the-art review from a clinical perspective. *Front Aging Neurosci*. 2023;15:1132077. doi:10.3389/fnagi.2023.1132077
14. Zhao Z, Nelson AR, Betsholtz C, Zlokovic BV. Establishment and dysfunction of the blood-brain barrier. *Cell*. 2015;163:1064-1078. doi:10.1016/j.cell.2015.10.067
15. Shao X, Ma SJ, Casey M, D'Orazio L, Ringman JM, Wang D. Mapping water exchange across the blood-brain barrier using 3D diffusion-prepared arterial spin labeled perfusion MRI. *Magn Reson Med*. 2019;81:3065-3079. doi:10.1002/mrm.27632
16. Gold BT, Shao X, Sudduth TL, et al. Water exchange rate across the blood-brain barrier is associated with CSF amyloid-β 42 in healthy older adults. *Alzheimers Dement*. 2021;17:2020-2029. doi:10.1002/alz.12357
17. Zachariou V, Pappas C, Bauer CE, et al. Regional differences in the link between water exchange rate across the blood–brain barrier and cognitive performance in normal aging. *Geroscience*. 2024;46:265-282. doi:10.1007/s11357-023-00930-2
18. Shao X, Shou Q, Felix K, et al. Age-related decline in BBB function is more pronounced in males than females. *Elife*. 2024;13:RP96155. doi:10.7554/eLife.96155
19. Li Y, Ying Y, Yao T, et al. Decreased water exchange rate across blood–brain barrier in hereditary cerebral small vessel disease. *Brain*. 2023;146:3079-3087. doi:10.1093/brain/awac500
20. Ying Y, Li Y, Yao T, et al. Heterogeneous blood-brain barrier dysfunction in cerebral small vessel diseases. *Alzheimers Dement*. 2024;20:4527-4539. doi:10.1002/alz.13874
21. Ling C, Zhang J, Shao X, et al. Diffusion prepared pseudo-continuous arterial spin labeling reveals blood-brain barrier dysfunction in patients with CADASIL. *Eur Radiol*. 2023;33:6959-6969. doi:10.1007/s00330-023-09652-7
22. Goldwaser EL, Wang D, Adhikari BM, et al. Evidence of neurovascular water exchange and endothelial vascular dysfunction in schizophrenia: an exploratory study. *Schizophr Bull*. 2023;49:1325-1335. doi:10.1093/schbul/sbad057
23. Uchida Y, Kan H, Sakurai K, et al. APOE varepsilon4 dose associates with increased brain iron and beta-amyloid via blood-brain barrier dysfunction. *J Neurol Neurosurg Psychiatry*. 2022;93:772-778. doi:10.1136/jnnp-2021-328519
24. Li X, Wang X, Su L, Hu X, Han Y. Sino Longitudinal Study on Cognitive Decline (SILCODE): protocol for a Chinese longitudinal observational study to develop risk prediction models of conversion to mild cognitive impairment in individuals with subjective cognitive decline. *BMJ OPEN*. 2019;9:e28188. doi:10.1136/bmjopen-2018-028188
25. Bondi MW, Edmonds EC, Jak AJ, et al. Neuropsychological criteria for mild cognitive impairment improves diagnostic precision, biomarker associations, and progression rates. *J Alzheimers Dis*. 2014;42:275-289. doi:10.3233/JAD-140276
26. Spann SM, Shao X, Wang DJ, et al. Robust single-shot acquisition of high resolution whole brain ASL images by combining time-dependent 2D CAPIRINHA sampling with spatio-temporal TGV reconstruction. *Neuroimage*. 2020;206:116337. doi:10.1016/j.neuroimage.2019.116337
27. Yan L, Liu CY, Wong KP, et al. Regional association of pCASL-MRI with FDG-PET and PiB-PET in people at risk for autosomal dominant Alzheimer's disease. *Neuroimage Clin*. 2018;17:751-760. doi:10.1016/j.nicl.2017.12.003
28. Yu X, Shi R, Zhou X, et al. Correlations between plasma markers and brain Aβ deposition across the AD continuum: evidence from SILCODE. *Alzheimer's Dement*. 2024;20:6170-6182. doi:10.1002/alz.14084
29. Shao K, Hu X, Kleineidam L, et al. Amyloid and SCD jointly predict cognitive decline across Chinese and German cohorts. *Alzheimer's Dement*. 2024;20:5926-5939. doi:10.1002/alz.14119
30. Bucci M, Savitcheva I, Farrar G, et al. A multisite analysis of the concordance between visual image interpretation and quantitative analysis of [(18)F]flutemetamol amyloid PET images. *Eur J Nucl Med Mol Imaging*. 2021;48:2183-2199. doi:10.1007/s00259-021-05311-5
31. Igartua JJ, Hayes AF. Mediation, moderation, and conditional process analysis: concepts, computations, and some common confusions. *Span J Psychol*. 2021;24:e49. doi:10.1017/SJP.2021.46
32. Zipser BD, Johanson CE, Gonzalez L, et al. Microvascular injury and blood–brain barrier leakage in Alzheimer's disease. *Neurobiol Aging*. 2007;28:977-986. doi:10.1016/j.neurobiolaging.2006.05.016
33. Ryu JK, McLarnon JG. A leaky blood-brain barrier, fibrinogen infiltration and microglial reactivity in inflamed Alzheimer's disease brain. *J Cell Mol Med*. 2009;13:2911-2925. doi:10.1111/j.1582-4934.2008.00434.x
34. Raja R, Rosenberg GA, Caprihan A. MRI measurements of Blood-Brain Barrier function in dementia: a review of recent studies. *Neuropharmacology*. 2018;134:259-271. doi:10.1016/j.neuropharm.2017.10.034
35. Montagne A, Barnes SR, Sweeney MD, et al. Blood-brain barrier breakdown in the aging human hippocampus. *Neuron*. 2015;85:296-302. doi:10.1016/j.neuron.2014.12.032
36. van de Haar HJ, Burgmans S, Jansen JF, et al. Blood-brain barrier leakage in patients with early Alzheimer disease. *Radiology*. 2016;281:527-535. doi:10.1148/radiol.2016152244
37. Preis L, Villringer K, Brosseron F, et al. Assessing blood-brain barrier dysfunction and its association with Alzheimer's pathology, cognitive

impairment and neuroinflammation. *Alzheimers Res Ther*. 2024;16:172. doi:10.1186/s13195-024-01529-1
38. Dyrna F, Hanske S, Krueger M, Bechmann I. The blood-brain barrier. *J Neuroimmune Pharmacol*. 2013;8:763-773. doi:10.1007/s11481-013-9473-5
39. Nedergaard M, Goldman SA. Glymphatic failure as a final common pathway to dementia. *Science*. 2020;370:50-56. doi:10.1126/science.abb8739
40. Yang J, Lunde LK, Nuntagij P, et al. Loss of astrocyte polarization in the tg-ArcSwe mouse model of Alzheimer's disease. *J Alzheimers Dis*. 2011;27:711-722. doi:10.3233/JAD-2011-110725
41. Zeppenfeld DM, Simon M, Haswell JD, et al. Association of perivascular localization of aquaporin-4 with cognition and Alzheimer disease in aging brains. *JAMA Neurol*. 2017;74:91-99. doi:10.1001/jamaneurol.2016.4370
42. Ashton NJ, Brum WS, Di Molfetta G, et al. Diagnostic accuracy of a plasma phosphorylated Tau 217 immunoassay for Alzheimer disease pathology. *JAMA Neurol*. 2024;81:255-263. doi:10.1001/jamaneurol.2023.5319
43. Arranz J, Zhu N, Rubio-Guerra S, et al. Diagnostic performance of plasma pTau217, pTau181, Aβ1-42 and Aβ1-40 in the LUMIPULSE automated platform for the detection of Alzheimer disease. *Alzheimers Res Ther*. 2024;16. doi:10.1186/s13195-024-01513-9
44. Therriault J, Servaes S, Tissot C, et al. Equivalence of plasma p-tau217 with cerebrospinal fluid in the diagnosis of Alzheimer's disease. *Alzheimers Dement*. 2023;19:4967-4977. doi:10.1002/alz.13026
45. Mattsson N, Andreasson U, Zetterberg H, Blennow K, SDNI Alzheimer, TASD For. Association of plasma neurofilament light with neurodegeneration in patients with Alzheimer disease. *JAMA Neurol*. 2017;74:557-566. doi:10.1001/jamaneurol.2016.6117
46. Kim KY, Shin KY, Chang K. GFAP as a potential biomarker for Alzheimer's disease: a systematic review and meta-analysis. *Cells (Basel, Switzerland)*. 2023;12:1309. doi:10.3390/cells12091309
47. Linnerbauer M, Wheeler MA, Quintana FJ. Astrocyte crosstalk in CNS inflammation. *Neuron*. 2020;108:608-622. doi:10.1016/j.neuron.2020.08.012

SUPPORTING INFORMATION

Additional supporting information can be found online in the Supporting Information section at the end of this article.

How to cite this article: Chen G, Li H, Shao X, et al. Decreased water exchange rate across the blood–brain barrier throughout the Alzheimer's disease continuum: Evidence from Chinese data. *Alzheimer's Dement*. 2025;21:e70089. https://doi.org/10.1002/alz.70089